Since January 2020 Elsevier has created a COVID-19 resource centre with free information in English and Mandarin on the novel coronavirus COVID-19. The COVID-19 resource centre is hosted on Elsevier Connect, the company's public news and information website.

Microbial Pathogenesis 170 (2022) 105685

Contents lists available at ScienceDirect

Microbial Pathogenesis

journal homepage: www.elsevier.com/locate/micpath

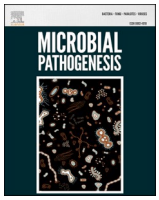

Moraxella occupied the largest proportion in the nasal microbiome in healthy children, which potential protect them from COVID-19

Xia Yu [a,1], Li Wang [a,1], XueMei Zheng [b,1], Yizhou Wen [c], Zhirong Zhang [d], Lingxia Fan [c], Qin Zhou [a], Xiao Yang [e], Binqian Xue [a], Yonghong Lin [e,*]

[a] Department of Clinical Laboratory, Chengdu Women's and Children's Central Hospital, School of Medicine, University of Electronic Science and Technology of China, Chengdu, PR China
[b] School of Medicine, University of Electronic Science and Technology of China, Chengdu, PR China
[c] Department of Pediatric Cardiology, Chengdu Women's and Children's Central Hospital, School of Medicine, University of Electronic Science and Technology of China, Chengdu, PR China
[d] Key Laboratory of Molecular Biology for Infectious Diseases, Ministry of Education, Chongqing Medical University, Chongqing, PR China
[e] Department of Obstetrics and Gynecology, Chengdu Women's and Children's Central Hospital, School of Medicine, University of Electronic Science and Technology of China, Chengdu, PR China

ARTICLE INFO

Keywords:
Upper respiratory tract
Microbiome
Moraxella
Children
COVID-19

ABSTRACT

Background: In the prevalence of COVID-19, infection symptoms are different in children and adults. In this study to investigate the differences in the upper respiratory tract microbiome profile between healthy children and adults and to explore which microbiome protect them from COVID-19.
Methods: Thirty healthy children and 24 healthy adults were enrolled between October 2020 and January 2021. Nasal and throat swabs were obtained at enrollment, and DNA was extracted. We performed 16S rDNA sequencing to compare the alpha and beta diversity of the nasal and throat microbiomes between children and adults and assessed potential microbiome biomarkers.
Results: In the nasal microbiome, there were significant differences between healthy children and adults, and *Moraxella* occupied the largest proportion in healthy children. Notably, there was no significant difference between healthy children and adults in the throat microbiome, and it was predominated by *Firmicutes*. In the function analysis, compared with adults, there was increased enrichment in pathways related to amino acid metabolism and lipid metabolism, in children.
Conclusions: In the upper respiratory tract microbiome profiles, *Moraxella* may be involved in protecting children from COVID-19 infections and may be involved the amino acid metabolism and lipid metabolism.

1. Introduction

Coronavirus disease 2019 (COVID-19) is defined as a disease resulting from severe acute respiratory syndrome coronavirus 2 (SARS-CoV-2) infection. SARS-CoV-2 can colonize the respiratory tract, especially the upper respiratory tract (URT), and then cause some common respiratory symptoms [1–4]. It's worth noting that infection rates in children are lower than in adults and they also have milder symptoms [5–7]. Many studies have been devoted to explaining this result [8,9]. However, there is little research from the differences in the upper respiratory tract microbiome composition between children and adults to explain this phenomenon.

It is well known that there are some interactions between viruses and bacteria [10]. During the COVID-19 epidemic, studies from many countries have reported that the incidences of various respiratory diseases have changed [11–13] and in the patient, whom infected with COVID-19, that the URT microbiome profile is characterized by *Acinetobacter, Chryseobacterium, Burkholderia, Brevundimonas, Sphingobium,* and *Enterobacteriaceae* [14–16]. Therefore, it is necessary to explore the different responses of children and adults to COVID-19 from the microbiome profile perspective. And the URT as the first line of defense in the respiratory system, analyzing the differences in the URT

* Corresponding author. Department of Obstetrics and Gynecology, Chengdu Women's and Children's Central Hospital, School of Medicine, University of Electronic Science and Technology of China, No.1617 Ri Yue Street, Chengdu, Sichuan, 611731, China.
E-mail address: linyhcd2011@163.com (Y. Lin).
[1] Co-first author.

https://doi.org/10.1016/j.micpath.2022.105685
Received 14 January 2022; Received in revised form 9 July 2022; Accepted 15 July 2022
Available online 21 July 2022

microbiome profile between children and adults is valuable.

Therefore, in this study, we explored the composition of the URT microbiota between healthy children and adults using 16S rDNA sequencing of nasal and throat swabs. This pilot study revealed that there were significant differences between healthy children and adults in the nasal microbiome, and *Moraxella* occupied the largest proportion in healthy children. These findings may provide a potential basis to explore which microbiome protect children from COVID-19.

2. Materials and methods

2.1. Study population

This study enrolled 30 children and 24 adults from Chengdu Women's and Children's Central Hospital from October 2020 to January 2021. The inclusion criteria were as follows: (1) normal routine physical examination and normal development; (2) no history of respiratory disease within 1 month before the sample was collected; and (3) no antibiotic use or any microecological agent exposure in the past month. In addition, subjects volunteered to participate.

This study was approved by the Medical Ethics Committee of Chengdu Women's and Children's Central Hospital (REC.2020.34). All subjects provided written informed consent.

2.2. Sample collection and DNA extraction

Samples were taken from children and adults using nasal and throat swabs. The nasal swabs were extended into the nasal cavity and rotated from inside to outside of the nasal mucosa. The throat swabs were rotated on the posterior wall of the pharynx to avoid contact with saliva, the tongue and the oral mucosa. After successful sample collection, the head of the swab was placed into a sterilized cryopreservation tube and stored at −80 °C.

DNA was extracted using the E.Z.N.A.® Stool DNA kit (D4015, Omega, Inc., USA) according to the manufacturer's instructions, and then all DNA samples were frozen at −80 °C for further processing.

2.3. 16S rDNA PCR and sequencing

The extracted DNA samples were amplified at the V3–V4 hypervariable region of the 16S rDNA gene by PCR with the following primers: 341F: 5′-CCTACGGGNGGCWGCAG-3′, 805R: 5′-GACTACHVGGGTATCTAATCC-3′). PCR was performed in a total reaction volume of 25 μl, including 25 ng of template DNA, 12.5 μl PCR premix, 2.5 μl of each primer, and PCR-grade water to adjust the volume. The PCR conditions to amplify the prokaryotic 16S fragments consisted of an initial denaturation at 98 °C for 30 s; 32 cycles of denaturation at 98 °C for 10 s, annealing at 54 °C for 30 s, and extension at 72 °C for 45 s; and then a final extension at 72 °C for 10 min. Two percent agarose gel electrophoresis was used to confirm the PCR products. To exclude the possibility of false-positive PCR results, ultrapure water was used as a negative control instead of a sample solution in the DNA extraction process. The PCR products were purified by AMPure XT beads (Beckman Coulter Genomics, Danvers, MA, USA) and quantified by Qubit (Invitrogen, USA). The sequencing used amplicon pools, and the Agilent 2100 Bioanalyzer (Agilent, USA) and the Library Quantification Kit for Illumina (Kapa Biosciences, Woburn, MA, USA) were used to evaluate the size and quantity of the amplicon library, respectively. The NovaSeq PE250 platform was used to complete the library sequence.

2.4. Sequencing analysis

According to the manufacturer's recommendations provided by LC-Bio, the samples were sequenced on the Illumina NovaSeq platform. Paired-end reads were assigned to the samples based on their unique barcode and truncated by cutting off the barcode and primer sequence. Paired-end reads were merged using FLASH. Quality filtering of the raw reads was performed under specific filtering conditions to obtain high-quality clean tags according to the fqtrim (v0.94). Chimeric sequences were filtered using Vsearch software (v2.3.4). After dereplication using DADA2, we obtained a feature table and feature sequence. Alpha diversity and beta diversity were calculated by random normalization to the same sequences. Then, according to the SILVA (release 132) classifier, feature abundance was normalized using the relative abundance of each sample. Alpha diversity was applied to analyze the complexity of species diversity for a sample through 5 indices, including Chao1, observed species, Good's coverage, and the Shannon and Simpson indices, and all these indices were calculated with QIIME2. Beta diversity was calculated by QIIME2, and the graphs were drawn by the R package. Blast was used for sequence alignment, and the feature sequences were annotated with the SILVA database for each representative sequence. Other diagrams were implemented using the R package (v3.5.2).

2.5. Statistics

The median and interquartile range are used to show all numerical data. Continuous data were divided into normal or nonnormal distributions by the Shapiro-Wilk test. Normally distributed data were compared with Student's *t*-test, and nonnormally distributed data were compared with the Mann-Whitney *U* test and Wilcoxon matched-pairs signed rank test between 2 groups. Linear discriminant analysis effect size (LEfSe) assessment was used to evaluate the proportions of the URT microbiome. For beta diversity, the URT microbiome composition was calculated by the UniFrac metric between samples, principal coordinate analysis (PCoA) was exploited to show the results, and permutational multivariate analysis of variance (PERMANOVA) was used for the statistical analysis. A p value of <0.05 was considered statistically significant.

3. Results

3.1. Study population and sample information

This study enrolled 30 children (17 males and 13 females) and 24 adults (4 males and 20 females) from Chengdu Women's and Children's Central Hospital from October 2020 to January 2021. The characteristics of the study population are shown in Table 1. According to the age and sampling site, we defined 6 groups as follows: NP_C, OP_C, NP_A, OP_A, A and C. Eleven nasal samples from children were excluded because target bands were not detected, and a total of 19 samples underwent high-quality 16S DNA sequencing detection. In our present investigation, 4620601 16sDNA reads were obtained. The composition of the respiratory microflora of all samples at the phylum and genus levels is shown in Fig. 1.

3.2. Nasal microbiome composition between healthy children and adults

In our study, to explore the characterization of the nasal microbiome in healthy children and adults, we compared the alpha diversity and beta diversity between the NP_C and NP_A groups using 16S DNA sequencing. The relative taxon abundance results showed that

Table 1
Characteristics of study population.

Parameter	Children	Adults
No. of participants	30	24
Age mean (rang), years	5(0.6–14)	25(18–30)
Gender		
Female	13	20
Male	17	4

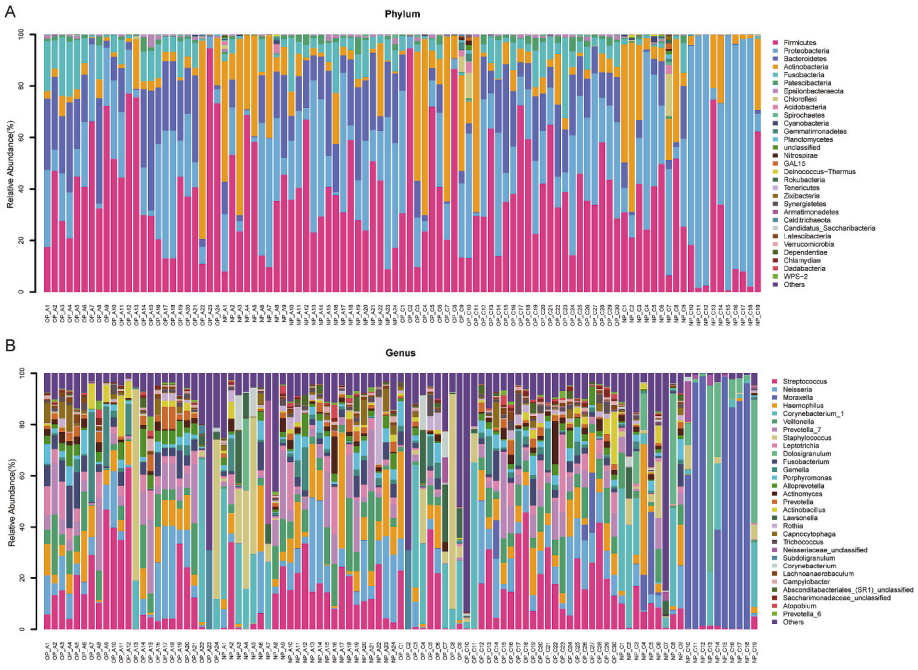

Fig. 1. The 30 most abundant bacterial (A) phyla, (B) genera in all samples.

Proteobacteria, Firmicutes, Actinobacteria, and *Bacteroidetes* were predominant in the 2 groups at the phylum level (Fig. 2A). Moreover, compared with the NP_C group, there was a significant increase in the relative abundance of *Bacteroidetes* and a slight decrease in the relative abundance of *Proteobacteria* in the NP_A group ($p = 0.0001$, $p = 0.04$, respectively). Surprisingly, at the genus level, *Moraxella* occupied the largest proportion in the NP_C group (37.21%) and only 0.06% in the NP_A group ($p = 0.0145$) (Fig. 2D). There was no significant difference in the observed species and the Chao 1 index, while the Shannon index and Simpson index were significantly higher in the NP_A group than in the NP_C group for the alpha diversity ($p = 0.012$, $p = 0.0023$). Furthermore, there were significant differences in nasal microbiome composition between the NP_A group and NP_C group as measured by the unweighted (PERMANOVA, $p = 0.002$) and weighted (PERMANOVA, $p = 0.001$) UniFrac (Fig. 3A and Fig. 3D). In addition, these significant differences were confirmed based on the LEfSe analysis, as indicated by the linear discriminate analysis (LDA). A significant increase in the relative abundances of *Leptotrichia* (*Fusobacteria*), *Streptococcus* (*Firmicutes*), *Haemophilus* (*Proteobacteria*), *Neisseria* (*Proteobacteria*), *Veillonella* (*Firmicutes*) and *Prevotella* (*Bacteroidetes*), but a significant reduction in *Dolosigranulum* (*Firmicutes*), *Moraxella* (*Proteobacteria*), and *Corynebacterium* (*Actinobacteria*) was observed in the

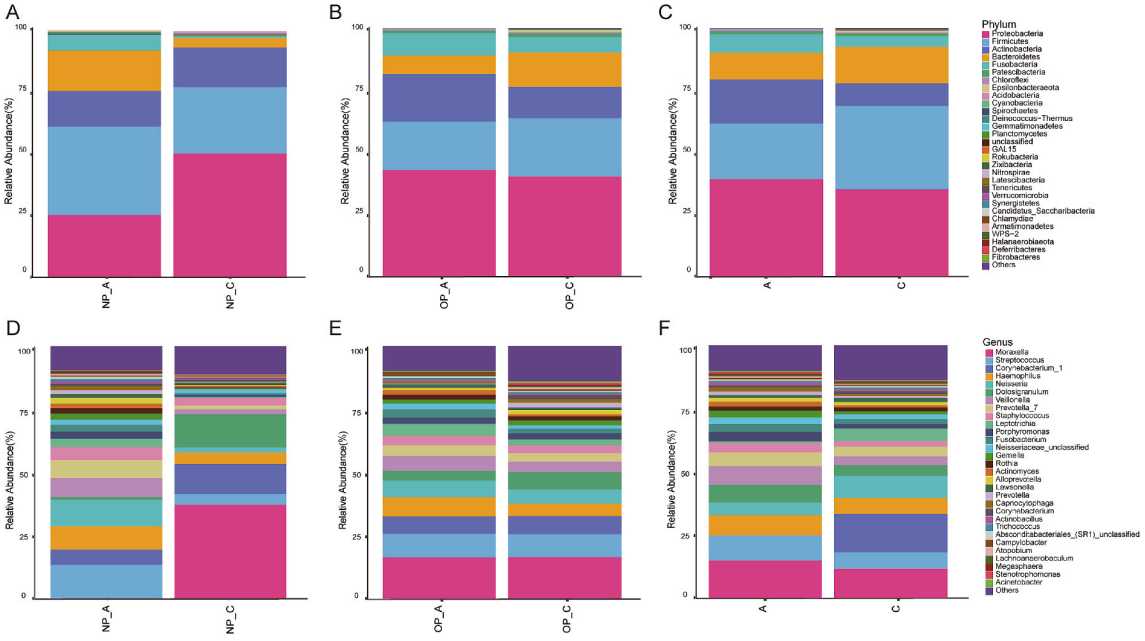

Fig. 2. Comparison of the relative abundances at the phylum level and genus level between the heathy children and adults in (A–C) NP_A vs. NP_C, OP_A vs. OP_C, A vs. C, (D–F) NP_A vs. NP_C, OP_A vs. OP_C, A vs. C. NP_A, adults' nasal swabs; NP_C, children's nasal swabs; OP_A, adults' throat swabs; OP_C, children's throat swabs; A, healthy adults; C, healthy children.

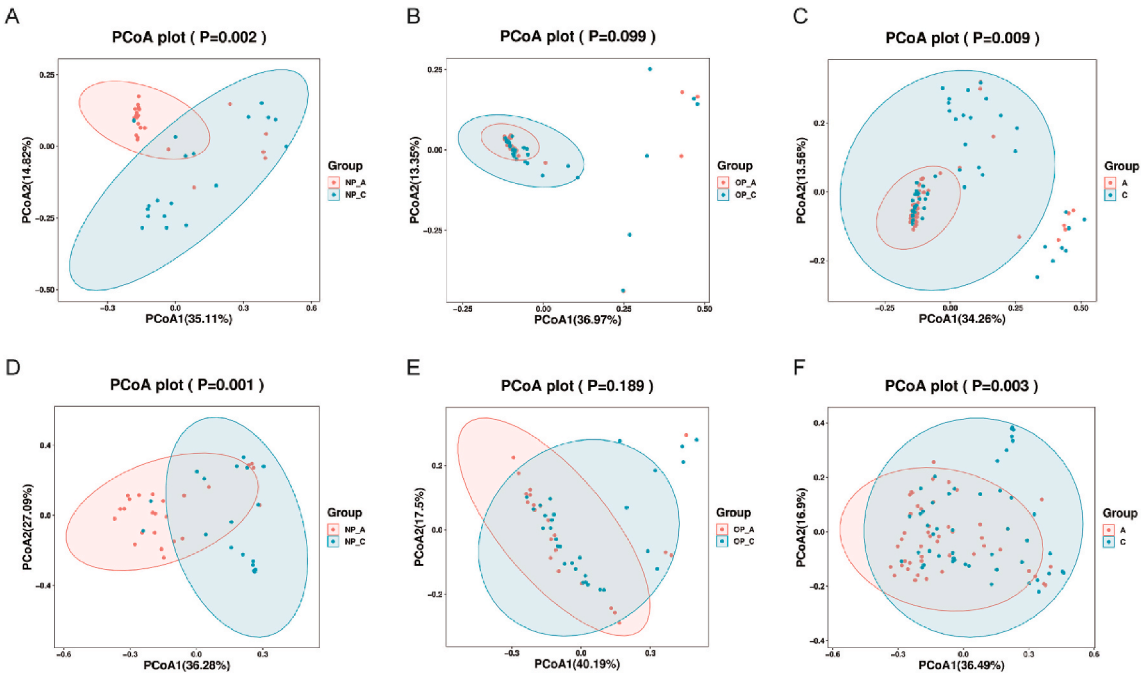

Fig. 3. Microbiome community analysis. PCoA of beta diversity using the unweighted UniFrac distances for (A–C) NP_A vs. NP_C, OP_A vs. OP_C, A vs. C, and the weighted UniFrac distances for (D–F) NP_A vs. NP_C, OP_A vs. OP_C, A vs. C. *p* values were calculated using the PERMANOVA. PCoA, principal coordinate analysis; permutational multivariate analysis of variance, PERMANOVA.

NP_A group in comparison with the NP_C group (LDA scores ($\log_{10}$) >4, $p < 0.05$) (Supplementary Figs. 1A and C).

3.3. Throat microbiome composition between healthy children and adults

To identify the throat microbiome profiles in healthy children and adults, the alpha diversity and beta diversity were compared between the OP_C and OP_A groups. The relative taxon abundances of both groups were predominated by *Firmicutes, Proteobacteria, Bacteroidetes, Actinobacteria,* and *Fusobacteria* at the phylum level, but there was no significant difference between the 2 groups ($p = 0.63$, $p = 0.40$, $p = 0.05$, $p = 0.08$, and $p = 0.12$, respectively) (Fig. 2B). We also investigated the relative abundance of the signature microbiome in the taxa at the genus level (Fig. 2E). *Streptococcus* and *Neisseria* were predominant in the microbiome. The observed species ($p = 0.90$), Chao1 index ($p = 0.92$), Shannon index ($p = 0.47$), and Simpson index ($p = 0.63$) showed no significant differences between the 2 groups. Furthermore, there were also no significant differences in the throat microbiome composition as measured by the unweighted (PERMANOVA, $p = 0.099$) and weighted (PERMANOVA, $p = 0.189$) UniFrac method (Fig. 3B and E). In addition, we also analyzed the significant differences based on LEfSe analysis, as indicated by the LDA levels. (LDA scores ($\log_{10}$) >4, $p < 0.05$) (Supplementary Figs. 1B and 1D).

3.4. Upper respiratory tract microbiome composition between children and adults

To analyze the microbiome profile of the URT, we integrated the nasal and throat microbiome samples from children and adults to form groups A and C, respectively. Their relative taxon abundances mainly included *Firmicutes, Proteobacteria, Bacteroidetes, Actinobacteria,* and *Fusobacteria* at the phylum level. Compared with the C group, there was a significant increase in the relative abundances of *Bacteroidetes and Fusobacteria* in the A group ($p = 0.0002$ and $p = 0.0032$, respectively) (Fig. 2C). At the genus level, *Streptococcus* accounted for the largest proportion in the A group, with no significant difference between the 2 groups ($p = 0.21$), but *Moraxella* had the highest proportion in the C group, and there was a significant increase compared with that in the A group ($p = 0.001$) (Fig. 2F). The alpha diversity showed no significant differences based on the observed species ($p = 0.67$), the Chao 1 index ($p = 0.69$), the Shannon index ($p = 0.08$), and the Simpson index ($p = 0.08$). In contrast, there were significant differences in the URT microbiota composition between the A group and C group as measured by the unweighted (PERMANOVA, $p = 0.009$) and weighted (PERMANOVA, $p = 0.003$) UniFrac (Fig. 3C and F). In addition, compared with the C group, these significant differences were confirmed by LEfSe analysis. A significant increase in the relative abundances of *Actinomyces* (*Actinobacteria*), *Leptotrichia* (*Fusobacteria*), *Porphyromonas* (*Bacteroidetes*), *Haemophilus* (*Proteobacteria*), *Neisseriaceae* (*Proteobacteria*), *Prevotella* (*Bacteroidetes*), *Veillonella* (*Firmicutes*), *Capnocytophaga* (*Bacteroidetes*), *Fusobacterium* (*Fusobacteria*), and *Alloprevotella* (*Bacteroidetes*), but a significant reduction in *Dolosigranulum* (*Firmicutes*), *Corynebacteriaceae* (*Actinobacteria*), *Moraxella* (*Proteobacteria*), and *Streptobacillus* (*Fusobacteria*) was observed in the A group (LDA scores ($\log_{10}$) >4, $p < 0.05$, Fig. 4).

3.5. KEGG pathway were distinct between URT microbiome of children and adults

Based on the phylogenetic investigation of communities by reconstruction of unobserved states 2 (PICRUSt 2), KEGG pathways were predicted between the microbiomes of healthy children and adults. The results revealed 39 different KEGG pathways between NP-C group and NP-A group. And compared with the C group, 18 different KEGG pathways were identified in the A group. Increased enrichment in pathways related to amino acid metabolism lipid metabolism were shown in the NP-C group and C group (Fig. 5).

4. Discussion

Owing to the interaction between viruses and bacteria and the URT as the first line of defense in the respiratory system, to explain the varying symptoms between children and adults infected with COVID-19 by analyzing the composition of URT microbiome profile is valuable. To

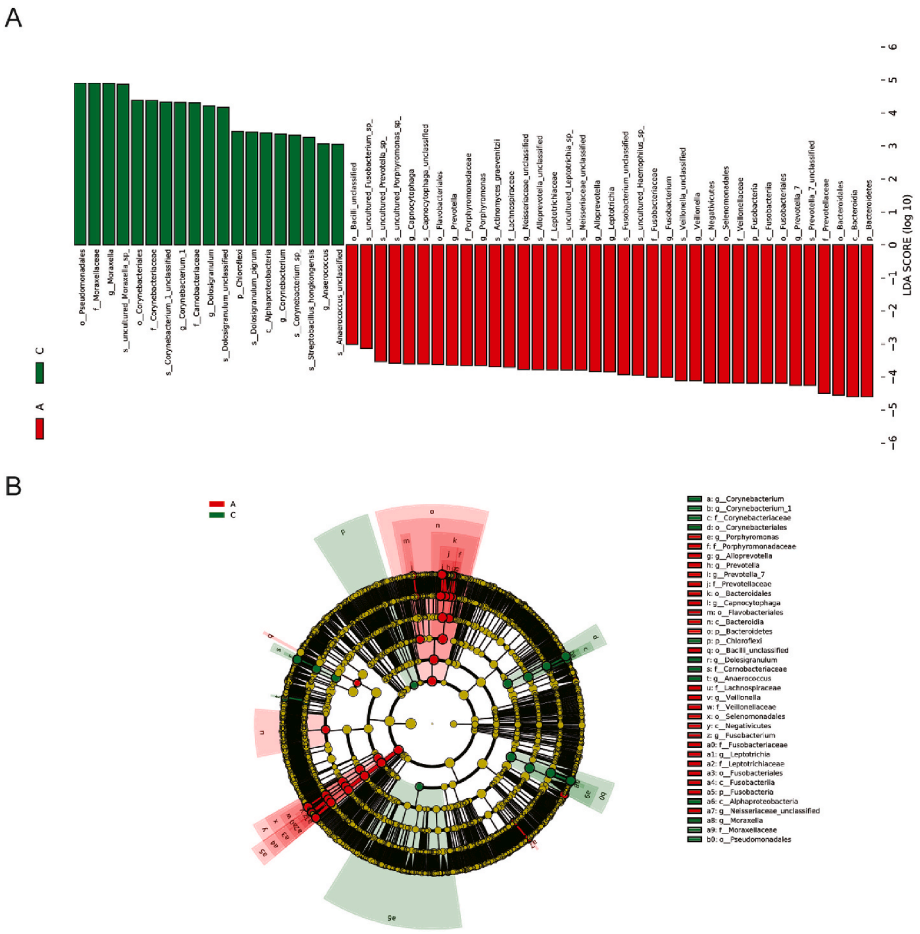

Fig. 4. LEfSe analysis between A and C groups. (A) Histogram of the LDA scores, (B) Cladogram. The circles radiating from the inside to the outside represent the classification level from the boundary (a single circle) to the genus (or species). Each small circle at different classification levels represents a classification at that level, and the diameter of the small circle is proportional to the relative abundance. p, phylum; c, class; o, order; f, family; g, genus.

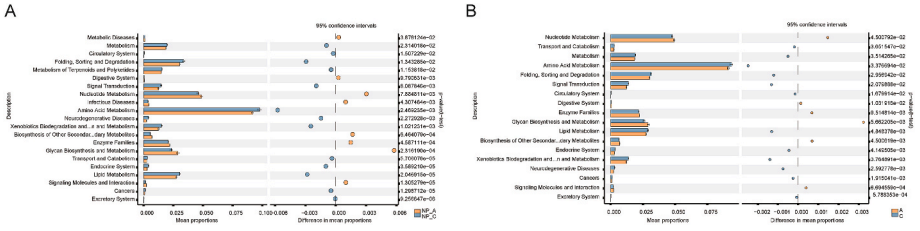

Fig. 5. Functional prediction of microbiome genes and analysis of differences in metabolic pathways based on KEGG pathways. Significant difference of KEGG pathways were shown in the extended error bar plot between (A) NP_A vs. NP_C, (B) A vs. C.

clarify this issue, we examined nasal and throat swabs from healthy children and adults using 16S DNA sequencing. Our study found that there was no significant difference in the throat microbiome between them. However, there were significant differences in the composition of the nasal microbiome at the genus level and dominated by *Moraxella* in healthy children.

There have been many reports about the microbiota is important for host resistance to respiratory infections, especially the role of the gut microbiota [1]. During the current COVID-19 pandemic, Zuo et al. revealed significant associations between defined gut microbiota states and an increased risk of severe disease upon respiratory viral infection in COVID-19 patients [17]. About the respiratory flora, in the most recent articles published by Xu et al. which examined the microbiome profile in the URT of children during the early infection stages of COVID-19 [14], consistent with our results, particular differences were found in the children's nasal microbiome at the genus level and *Moraxella* accounted for the largest proportion. There are no definite experimental results to confirm that *Moraxella* is resistant to COVID-19 infection. However, Biesbroek et al. reported fewer respiratory infections in children with nasopharyngeal colonisation by *Moraxella* [18,19]. And Lagier JC et al. performed PCR experiments using nasal swabs and found that the proportion of *Moraxella* decreased in deceased COVID-19 patients, compared with the patients with a favorable outcome, asymptomatic patients and COVID-19 negative subjects [20]. One explanation for this might be the SARS-CoV-2 entry receptor can be suppressed by commensal human microbiota [21]. Metagenomic analysis of RNA sequencing data showed a significant decrease in commensal bacteria as the number of days of COVID-19 infection increased [22].There have been reported that *Moraxella* as a core genus of nasal commensal bacteria in children [23,24], and this is in line with our findings. In

addition, *Moraxella* can affect the immune system of the respiratory tract [25]. Sönnerborg A et al. demonstrated that *Moraxella* correlated inversely to inflammation marker CRP and D-dimer [26]. These results suggest that *Moraxella* may be associated with better outcomes after COVID-19 infection. Therefore, we speculate that *Moraxella* may play a role of protecting children in the background of COVID-19.

In order to explore the other possible mechanisms of the protective effect of *Moraxella*. We used KEGG pathway to do functional analysis and the results showed that these different of nasal microbiome involved the lipid metabolism and amino acid metabolism in the children. Zhang S et al. have uncovered that the decrease of *Moraxella* can lead to disorder of lipid metabolism and amino acid metabolism [27]. And Boral et al. revealed that the rational intake of polyunsaturated fatty acids or supplements might prevent COVID-19 infection and lessen the complications in COVID-19 [28]. Such results could be due to polyunsaturated fatty acids control the function of two SARS-CoV-2 entry gateways: the angiotensin-converting enzyme-2 and cellular protease transmembrane protease serine-2 [29], and docosahexaenoic acid involved in suppressing inflammation and augment phagocytosis [30], moreover, eicosapentaenoic acid produced prostaglandins of 3 series, leukotrienes of 5 series, and thromboxane A3 displayed anti-inflammatory, vasodilatory, and platelet anti-aggregatory effects [31]. Beyond that, Ansone et al. have exhibited that amino acid metabolism, especially the tryptophan (tryptophan, kynurenine, and 3-hydroxy-DL-kynurenine) and arginine (citrulline and ornithine) metabolism, was also significantly associate with the clinical severity of COVID-19 using longitudinal targeted metabolomics analysis [32]. And results have been reported that all or single essential amino acid deprivation can upregulate ACE2 expression, such as leucine deprivation increased ACE2 expression through transcription factors, MAF bZIP transcription factor B (MAFB) or MAF bZIP transcription factor F (MAFF), acted downstream of GCN2 [33]. Chen W et al., have demonstrated that amino acid metabolism can maintain and regulate the immune function of macrophages in response to viral infection [34]. Therefore, *Moraxella* correlated inversely to inflammation marker may be correlated with amino acid metabolism pathways. However, more experiments and evidence are needed to support this possibility.

There are several limitations to this study. On the one hand, the sample size was small in this study. Therefore, further research needs to carry out a large-scale study from multiple regions to confirm the main findings of our results. On the other hand, to clarify the protect effect of *Moraxella* in children, further study of *Moraxella* is necessary in animal and cellular models infected with COVID-19.

Funding

This work was supported by Chengdu science and technology bureau: technology innovation research and development project [grant number 2020-YF05-00200-SN] and Chengdu medical research project [grant number 2020216].

CRediT authorship contribution statement

Xia Yu: Methodology, Software, Writing – original draft. **Li Wang:** Methodology, Writing – original draft. **XueMei Zheng:** Writing – review & editing. **Yizhou Wen:** Methodology, Software. **Zhirong Zhang:** Methodology. **Lingxia Fan:** Methodology. **Qin Zhou:** Methodology. **Xiao Yang:** Software. **Binqian Xue:** Software. **Yonghong Lin:** Conceptualization, Supervision.

Conflicts of interest

The authors declare that there is no conflict of interest.

Data availability

The authors do not have permission to share data.

Acknowledgements

We thank AJE Academic Services (https://www.aje.cn) for English-language editing and review services.

Appendix A. Supplementary data

Supplementary data to this article can be found online at https://doi.org/10.1016/j.micpath.2022.105685.

References

[1] X.W. Xu, X.X. Wu, X.G. Jiang, K.J. Xu, L.J. Ying, C.L. Ma, et al., Clinical findings in a group of patients infected with the 2019 novel coronavirus (SARS-Cov-2) outside of Wuhan, China: retrospective case series, BMJ 368 (2020) m606, https://doi.org/10.1136/bmj.m606.

[2] N. Chen, M. Zhou, X. Dong, J. Qu, F. Gong, Y. Han, et al., Epidemiological and clinical characteristics of 99 cases of 2019 novel coronavirus pneumonia in Wuhan, China: a descriptive study, Lancet 395 (2020) 507–513, https://doi.org/10.1016/S0140-6736(20)30211-7.

[3] M. Shi, L. Chen, Y. Yang, J. Zhang, J. Xu, G. Xu, et al., Analysis of clinical features and outcomes of 161 patients with severe and critical COVID-19: a multicenter descriptive study, J. Clin. Lab. Anal. 34 (2020), e23415, https://doi.org/10.1002/jcla.23415.

[4] B.G. Madas, P. Füri, Á. Farkas, A. Nagy, A. Czitrovszky, I. Balásházy, et al., Deposition distribution of the new coronavirus (SARS-CoV-2) in the human airways upon exposure to cough-generated droplets and aerosol particles, Sci. Rep. 10 (2020), 22430, https://doi.org/10.1038/s41598-020-79985-6.

[5] Z. Wu, J.M. McGoogan, Characteristics of and important lessons from the coronavirus disease 2019 (COVID-19) outbreak in China: summary of a report of 72314 cases from the Chinese center for disease control and prevention, JAMA 323 (2020) 1239–1242, https://doi.org/10.1001/jama.2020.2648. :.

[6] G. Onder, G. Rezza, S. Brusaferro, Case-Fatality rate and characteristics of patients dying in relation to COVID-19 in Italy, JAMA 323 (2020) 1775–1776, https://doi.org/10.1001/jama.2020.4683, dio:.

[7] K.A.M. Gaythorpe, S. Bhatia, T. Mangal, H.J.T. Unwin, N. Imai, G. Cuomo-Dannenburg, et al., Children's role in the COVID-19 pandemic: a systematic review of early surveillance data on susceptibility, severity, and transmissibility, Sci. Rep. 11 (2021), 13903, https://doi.org/10.1038/s41598-021-92500-9.

[8] F. Midulla, L. Cristiani, E. Mancino, What do differences in case fatality ratios between children and adults tell us about COVID-19? Eur. Respir. J. 56 (2020), 2001601 https://doi.org/10.1183/13993003.01852-2020.

[9] S. Baggio, A.G. L'Huillier, S. Yerly, M. Bellon, N. Wagner, M. Rohr, et al., Severe acute respiratory syndrome coronavirus 2 (SARS-CoV-2) viral load in the upper respiratory tract of children and adults with early acute coronavirus disease 2019 (COVID-19), Clin. Infect. Dis. 73 (2021) 148–150, https://doi.org/10.1093/cid/ciaa1157, dio:.

[10] A.K. Berger, B.A. Mainou, Interactions between enteric bacteria and eukaryotic viruses impact the outcome of infection, Viruses 10 (2018) 19, https://doi.org/10.3390/v10010019.

[11] T. Itaya, Y. Furuse, K. Jindai, Does COVID-19 infection impact on the trend of seasonal influenza infection? 11 countries and regions, from 2014 to 2020, Int. J. Infect. Dis. 97 (2020) 78–80, https://doi.org/10.1016/j.ijid.2020.05.088, dio:.

[12] G. Iacobucci, Covid lockdown: England sees fewer cases of colds, flu, and bronchitis, BMJ 370 (2020) m3182, https://doi.org/10.1136/bmj.m3182.

[13] I. Kuitunen, M. Artama, L. Mäkelä, K. Backman, T. Heiskanen-Kosma, M. Renko, Effect of social distancing due to the COVID-19 pandemic on the incidence of viral respiratory tract infections in children in Finland during early 2020, Pediatr. Infect. Dis. J. 39 (2020) e423–e427, https://doi.org/10.1097/inf.0000000000002845.

[14] R. Xu, P. Liu, T. Zhang, Q. Wu, M. Zeng, Y. Ma, et al., Progressive deterioration of the upper respiratory tract and the gut microbiomes in children during the early infection stages of COVID-19, J. Genet. Genom. (2021), https://doi.org/10.1016/j.jgg.2021.05.004.

[15] R. Xu, R. Lu, T. Zhang, Q. Wu, W. Cai, X. Han, et al., Temporal association between human upper respiratory and gut bacterial microbiomes during the course of COVID-19 in adults, Commun Biol 4 (2021) 240, https://doi.org/10.1038/s42003-021-01796-w.

[16] J. Fan, X. Li, Y. Gao, J. Zhou, S. Wang, B. Huang, et al., The lung tissue microbiota features of 20 deceased patients with COVID-19, J. Infect. 81 (2020) e64–e67, https://doi.org/10.1016/j.jinf.2020.06.047.

[17] T. Zuo, F. Zhang, G.C.Y. Lui, Y.K. Yeoh, A.Y.L. Li, H. Zhan, et al., Alterations in gut microbiota of patients with COVID-19 during time of hospitalization, Gastroenterology 159 (2020) 944–955, https://doi.org/10.1053/j.gastro.2020.05.048, e8.

[18] R.L. Marsh, M. Kaestli, A.B. Chang, M.J. Binks, C.E. Pope, L.R. Hoffman, et al., The microbiota in bronchoalveolar lavage from young children with chronic lung

disease includes taxa present in both the oropharynx and nasopharynx, Microbiome 4 (2016) 37, https://doi.org/10.1186/s40168-016-0182-1.
[19] W.H. Man, M.A. van Houten, M.E. Merelle, A.M. Vlieger, M. Chu, N.J.G. Jansen, et al., Bacterial and viral respiratory tract microbiota and host characteristics in children with lower respiratory tract infections: a matched case-control study, Lancet Respir. Med. 7 (2019) 417–426, https://doi.org/10.1016/S2213-2600(18)30449-1.
[20] Tchoupou Saha Olf, G. Dubourg, A. Yacouba, V. Bossi, D. Raoult, J.-C. Lagier, Profile of the nasopharyngeal microbiota affecting the clinical course in COVID-19 patients, Front. Microbiol. 13 (2022), https://doi.org/10.3389/fmicb.2022.871627.
[21] A. Edwinson, L. Yang, J. Chen, M. Grover, Colonic expression of Ace2, the SARS-CoV-2 entry receptor, is suppressed by commensal human microbiota, Gut Microb. 13 (2021), 1984105, https://doi.org/10.1080/19490976.2021.1984105.
[22] Clinical findings in a group of patients infected with the 2019 novel coronavirus (SARS-Cov-2) outside of Wuhan, China: retrospective case series, BMJ 368 (2020) m792, https://doi.org/10.1136/bmj.m792.
[23] L.M. Verhagen, I.A. Rivera-Olivero, M. Clerc, M. Chu, J. van Engelsdorp Gastelaars, M.I. Kristensen, et al., Nasopharyngeal microbiota profiles in rural Venezuelan children are associated with respiratory and gastrointestinal infections, Clin. Infect. Dis. 72 (2021) 212–221, https://doi.org/10.1093/cid/ciaa015, dio:.
[24] H. Wang, W. Dai, X. Feng, Q. Zhou, H. Wang, Y. Yang, et al., Microbiota composition in upper respiratory tracts of healthy children in shenzhen, China, differed with respiratory sites and ages, BioMed Res. Int. 2018 (2018), 6515670, https://doi.org/10.1155/2018/6515670.
[25] J. Ackland, A. Watson, T.M.A. Wilkinson, K.J. Staples, Interrupting the conversation: implications for crosstalk between viral and bacterial infections in the asthmatic airway, Front Allergy 2 (2021), 738987, https://doi.org/10.3389/falgy.2021.738987.
[26] X. Bai, A. Narayanan, M. Skagerberg, R. Cena-Diez, C.G. Giske, K. Stralin, et al., Characterization of the upper respiratory bacterial microbiome in critically Ill COVID-19 patients, Biomedicines 10 (2022), https://doi.org/10.3390/biomedicines10050982.
[27] H. Qiu, H. Gao, F. Yu, B. Xiao, X. Li, B. Cai, et al., Perinatal exposure to low-level PBDE-47 programs gut microbiota, host metabolism and neurobehavior in adult rats: an integrated analysis, Sci. Total Environ. 825 (2022), 154150, https://doi.org/10.1016/j.scitotenv.2022.154150.
[28] P.K. Baral, M.T. Amin, M.M.O. Rashid, M.S. Hossain, Assessment of polyunsaturated fatty acids on COVID-19-associated risk reduction, Revista Brasileira de Farmacognosia (2021), https://doi.org/10.1007/s43450-021-00213-x.
[29] R.A. Ballout, D. Sviridov, M.I. Bukrinsky, A.T. Remaley, The lysosome: a potential juncture between SARS-CoV-2 infectivity and Niemann-Pick disease type C, with therapeutic implications, Faseb. J. 34 (2020) 7253–7264, https://doi.org/10.1096/fj.202000654R, dio:.
[30] S.R. Wassall, X. Leng, S.W. Canner, E.R. Pennington, J.J. Kinnun, A.T. Cavazos, et al., Docosahexaenoic acid regulates the formation of lipid rafts: a unified view from experiment and simulation, Biochim. Biophys. Acta Biomembr. 1860 (2018) 1985–1993, https://doi.org/10.1016/j.bbamem.2018.04.016, dio:.
[31] C.I. Bercea, G.S. Cottrell, F. Tamagnini, A.J. McNeish, Omega-3 polyunsaturated fatty acids and hypertension: a review of vasodilatory mechanisms of docosahexaenoic acid and eicosapentaenoic acid, Br. J. Pharmacol. 178 (2021) 860–877, https://doi.org/10.1111/bph.15336.
[32] L. Ansone, M. Briviba, I. Silamikelis, A. Terentjeva, I. Perkons, L. Birzniece, et al., Amino acid metabolism is significantly altered at the time of admission in hospital for severe COVID-19 patients: findings from longitudinal targeted metabolomics analysis, Microbiol. Spectr. (2021), e0033821, https://doi.org/10.1128/spectrum.00338-21.
[33] X. Hu, Y. Niu, P. Luo, F. Xiao, F. Yuan, H. Yin, et al., Amino acid sensor GCN2 promotes SARS-CoV-2 receptor ACE2 expression in response to amino acid deprivation, Commun Biol 5 (2022) 651, https://doi.org/10.1038/s42003-022-03609-0.
[34] T. Gauthier, W. Chen, Modulation of macrophage Immunometabolism: a new approach to fight infections, Front. Immunol. 13 (2022), 780839, https://doi.org/10.3389/fimmu.2022.780839.